

Cite this: *CrystEngComm*, 2011, **13**, 4658

www.rsc.org/crystengcomm

PAPER

Synthesis and characterizations of calcium germanate nanowires

L. Z. Pei,* Y. Yang, C. G. Fan, C. Z. Yuan, T. K. Duan and Qian-Feng Zhang

Received 16th January 2011, Accepted 20th April 2011

DOI: 10.1039/c1ce05070b

Crystalline calcium germanate nanowires with a diameter of 50–200 nm and length of several dozens of micrometres have been synthesized by a simple and facile hydrothermal process. X-ray diffraction and high-resolution transmission electron microscopy results show that the crystalline calcium germanate nanowires are mainly composed of tetragonal Ca_2GeO_4 , orthorhombic $\text{Ca}_2\text{Ge}_7\text{O}_{16}$ and triclinic CaGe_2O_5 phases. The role of different growth conditions demonstrates that the hydrothermal temperature, reaction time, compactness, Ca source materials and surfactants play an essential role in the formation and size of the calcium germanate nanowires. The nucleation and crystalline growth mechanism are proposed to explain the formation and growth of the calcium germanate nanowires. The photoluminescence spectrum of the calcium germanate nanowires shows three fluorescence emission peaks centered at 421 nm, 488 nm and 529 nm, exhibiting a promising potential for optical applications.

Introduction

During the past years, there has been an increasing interest in ternary oxide nanowires due to the fundamental scientific interest and the attempt to develop new applications based on their novel optical, electric, photocatalytic and sensing properties.^{1–3} Various types of ternary oxide nanowires, such as BaTiO_3 nanowires,⁴ $\text{Zn}_2\text{Ti}_3\text{O}_8$ nanowires⁵ and Zn_2SnO_4 nanowires^{6,7} have been synthesized by low temperature solution processes, template methods and thermal evaporation processes, respectively. It has been shown that some ternary oxide nanostructures have better properties than binary oxide nanostructures in electron and gas sensors.^{8,9} One advantage of the ternary oxide nanostructures is that their properties can be efficiently tuned by adjusting their shapes and compositions.¹⁰ The successful synthesis of complex ternary oxide nanostructures with stoichiometric compositions and controllable morphologies requires more deliberate growth control.

In ternary oxide nanowires, ternary germanate nanowires have also attracted great attention as important nanomaterials for the application of electrochemical sensors, optical devices and catalysts.^{11–14} Several kinds of germanate nanowires, such as Zn_2GeO_4 nanowires,^{15,16} PbGeO_3 nanowires¹⁷ and strontium germanate nanowires,¹⁸ have been reported previously. Very recently, ternary germanate 1D nanomaterials have been synthesized by us, using a simple hydrothermal deposition route with GeO_2 , copper foil and zinc foil as the starting material and

deposition substrates, respectively, and good photoluminescence, electrochemical characteristics were observed.^{14,19,20} Therefore, it is of great significance to successfully synthesize novel species of germanate nanowires for potential applications in nanoscale devices by a simple and facile synthesis process. Bulk calcium germanate is an excellent optical material exhibiting strong fluorescence emission at 620, 700 and 800 nm.²¹ Recently, Perng *et al.*²² reported the synthesis and photoluminescence of amorphous $\text{Ca}_5\text{Ge}_2\text{O}_9$ nanowires by dehydrating the hydrated $\text{Ca}_5\text{Ge}_2\text{O}_9$ nanowires originated by submersing Ge nanoparticles into calcium hydroxide aqueous solution. However, Ge nanoparticles with the size ranging from 10 to 50 nm need firstly to be prepared by a vapor condensation technique, taking the complexity and expensive apparatus for the synthesis of the calcium germanate nanowires. It is particularly important that the crystalline materials may exhibit more special properties than amorphous materials. The $\text{Ca}_5\text{Ge}_2\text{O}_9$ nanowires are composed of an amorphous structure which cannot possess the unique properties of crystalline calcium germanate nanowires. Therefore, it is very desirable and significant to explore the simple and facile method for synthesizing crystalline calcium germanate nanowires for possible applications.

In the paper, crystalline calcium germanate nanowires have been successfully synthesized *via* a simple and facile hydrothermal process using GeO_2 and $\text{Ca}(\text{CH}_3\text{COO})_2 \cdot \text{H}_2\text{O}$ as the starting materials in the absence of any surfactant for the first time. The structure, morphology, size and photoluminescence properties of the calcium germanate nanowires have been fully analyzed by X-ray diffraction analysis, electron microscopy, Fourier transform infrared and photoluminescence spectra. The growth conditions dependence on the formation and possible formation mechanism of the calcium germanate nanowires have

School of Materials Science and Engineering, Institute of Molecular Engineering and Applied Chemistry, Key Lab of Materials Science and Processing of Anhui Province, Anhui University of Technology, Ma'anshan, Anhui, 243002, P. R. China. E-mail: lzpei1977@163.com; lzpei@ahut.edu.cn; Fax: +86-555-2311570; Tel: +86-555-2311570

also been investigated in detail. Proper selections and combinations of the growth conditions, such as reaction temperature, reaction time, compactness, Ca source materials and surfactants are the important aspects to achieve morphology and size control.

Experimental

High purity GeO_2 powders (purity: $\geq 99.99\%$) and Ca $(\text{CH}_3\text{COO})_2 \cdot \text{H}_2\text{O}$ (AR grade, purity: $\geq 99.0\%$) were purchased from Sinopharm Chemical Reagent Co., Ltd. of China. All the starting materials were used without further purification. In a typical procedure, 0.16 g GeO_2 and 0.54 g $\text{Ca}(\text{CH}_3\text{COO})_2 \cdot \text{H}_2\text{O}$ (GeO_2 is slightly soluble in water and its solubility in water is about 0.4 g/100 mL) were dissolved in 30 mL deionized water, respectively. The mole ratio of Ca : Ge is 2. The Ca $(\text{CH}_3\text{COO})_2 \cdot \text{H}_2\text{O}$ solution was added dropwise to GeO_2 solution under vigorous stirring. Then, the mixture was placed in a 100 mL autoclave with a Teflon liner. The autoclave was maintained at 80–180 °C for different reaction time. Subsequently, the autoclave was cooled naturally in air. The resulting white precipitates were filtered, washed with deionized water several times and dried at 60 °C in air. Finally, the white calcium germanate nanowire powders were obtained.

The obtained products were characterized by X-ray diffraction (XRD), scanning electron microscopy (SEM), transmission electron microscopy (TEM), high-resolution transmission electron microscopy (HRTEM), Fourier transform infrared spectroscopy (FTIR) and photoluminescence (PL) spectra. XRD pattern was carried out on a Bruker AXS D8 X-ray diffractometer equipped with a graphite monochromatized Cu-K α radiation ($\lambda = 1.5406 \text{ \AA}$). The samples were scanned at a scanning rate of $0.05^\circ \text{ s}^{-1}$ in the 2θ range of $20^\circ \sim 80^\circ$. SEM observation was performed using JEOL JSM-6490LV SEM with a 15 KV accelerating voltage. TEM and HRTEM samples were prepared by putting several drops of solution with calcium germanate nanowires onto a standard copper grid with a porous carbon film after the nanowire samples were dispersed into distilled water and treated for about 10 min using supersonic wave apparatus. TEM and HRTEM observations were performed using JEOL JEM-2100 TEM operating with 1.9 Å point-to-point resolution operating at 200 kV accelerating voltage with a GATAN digital photography system. FTIR spectroscopy (Perkin Elmer PE, WQF-410 spectrometer) was used at room temperature in the range of $450\text{--}4000 \text{ cm}^{-1}$ with a resolution of 4 cm^{-1} . PL measurement was carried out at room temperature using 235 nm as the excitation wavelength with a luminescence spectrometer (Cary Eclipse) in the range of 350–600 nm.

Results and discussion

The XRD pattern of the calcium germanate nanowires synthesized under the hydrothermal conditions of 180 °C for 24 h is shown in Fig. 1. By indexing the JCPDS cards, the main diffraction peaks for the calcium germanate nanowires can be assigned to the orthorhombic phase of Ca_2GeO_4 (JCPDS card No. 25-0137), orthorhombic phase of $\text{Ca}_2\text{Ge}_7\text{O}_{16}$ (JCPDS card No. 34-0286) and triclinic phase of CaGe_2O_5 (JCPDS card No. 23-0869). Besides the calcium germanate phases, a small amount

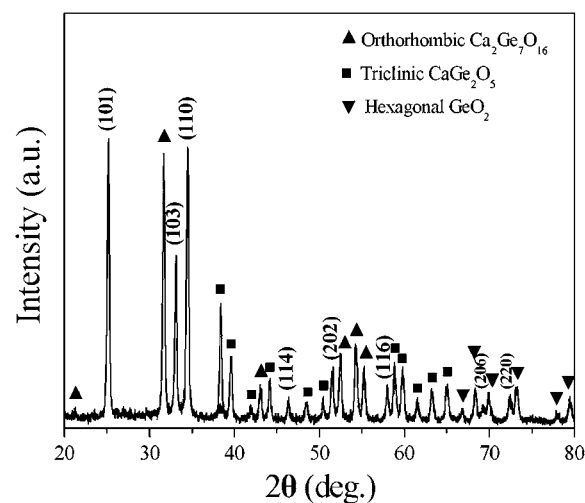


Fig. 1 X-ray diffraction pattern of the calcium germanate nanowires.

of hexagonal GeO_2 phase (JCPDS card No. 65-6772) exists in the nanowire sample which may originate from the residue of the starting materials. The crystalline structure of the calcium germanate nanowires is totally different from the amorphous $\text{Ca}_5\text{Ge}_2\text{O}_9$ nanowires synthesized by dehydrating the hydrated $\text{Ca}_5\text{Ge}_2\text{O}_9$ nanowires, originating by submersing Ge nanoparticles into calcium hydroxide aqueous solution.²¹

The general morphology and size of the calcium germanate nanowires are firstly observed by SEM which is shown in Fig. 2. SEM observations reveal that the calcium germanate nanowire products are composed of a large quantity of uniform and free-standing wirelike nanostructures with typical lengths in the range of several tens to several hundreds of micrometres. The diameter of the nanowires is about 50–200 nm. No other nanostructures or impurities are observed besides the calcium germanate nanowires, showing that the high purity calcium germanate nanowires can be obtained easily by the simple hydrothermal process. The high-magnification SEM image reveals that each nanowire is uniform throughout the diameter.

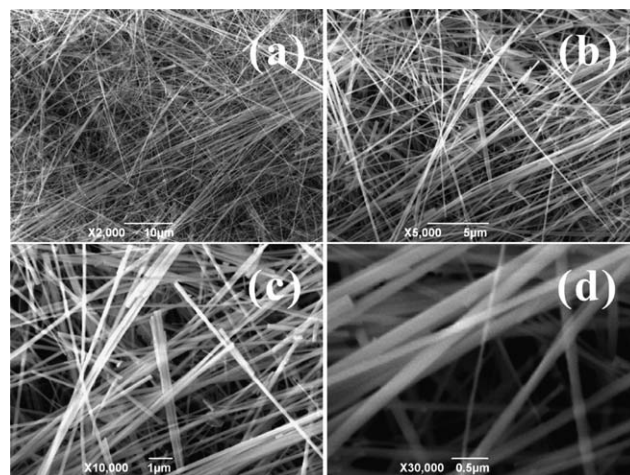


Fig. 2 SEM images of the calcium germanate nanowires with different magnifications.

The obtained calcium germanate nanowires consist of mixed germanate phases. In order to analyze whether the synthesis can be controlled to produce a single phase, the experiments using the raw materials with different Ca : Ge mole ratios at 180 °C for 24 h were conducted. The corresponding SEM images and XRD patterns are shown in Fig. 3. According to the SEM images of the products, it is found that the products are composed of nanowires with the diameter and length of 40–120 nm and several dozens of micrometres (Fig. 3a and c), respectively. XRD patterns of the products (Fig. 3b and d) show that the products also consist of mixed germanate phases with orthorhombic Ca_2GeO_4 , orthorhombic $\text{Ca}_2\text{Ge}_7\text{O}_{16}$ and triclinic CaGe_2O_5 structures. The morphology, size and structure of the calcium germanate nanowires obtained using the raw materials with different Ca : Ge mole ratios are almost the same as those of the calcium germanate nanowires obtained using the raw materials with a mole ratio of Ca : Ge = 2 (Fig. 1 and Fig. 2). The results show that only calcium germanate nanowires with mixed germanate phases can be synthesized which will be further proved by the following XRD patterns of the calcium germanate nanowires obtained from different hydrothermal conditions.

Fig. 4 shows typical low magnification TEM images of the calcium germanate nanowires which are similar to those of the SEM observations. The nanowires are straight and have a smooth surface. The diameter of the nanowires is uniform throughout the length. It is noticed that the calcium germanate nanowires have flat tips. The flat tips are similar to those of the CuGeO_3 nanowires prepared by us, using the hydrothermal deposition process.^{18,23}

The obtained calcium germanate nanowires consist of mixed germanate phases. The distribution of the three calcium germanate phases in the nanowires need to be understood so as to clarify if all three phases can be present in a single nanowire or a nanowire is always composed of single phase. HRTEM images

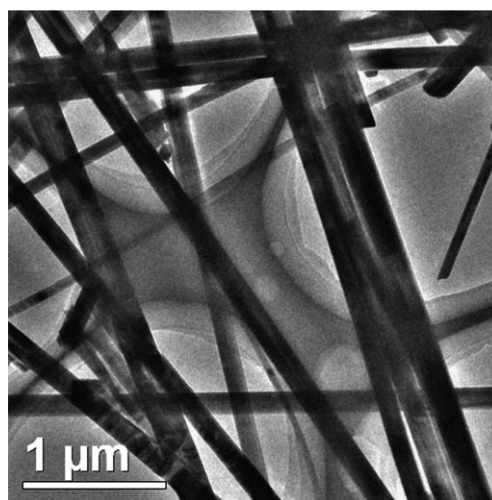


Fig. 4 TEM image of the calcium germanate nanowires.

can provide detailed structural information on the calcium germanate nanowires. Fig. 5a is the TEM image of the single calcium germanate nanowire and Fig. 5c–d are the corresponding HRTEM images from different parts of the nanowire. The HRTEM images show that the nanowires are composed of good crystalline structure. One can see a boundary in the HRTEM image at the edge of the calcium germanate nanowire which can be an interphase boundary (Fig. 5b). The interplanar spacing of the crystal is about 0.59 nm, 0.4 nm and 0.49 nm, respectively, from the inner part to the edge of the calcium germanate nanowire (Fig. 5b), according to the HRTEM measurement and the subsequent calculation by the software of Digital Micrograph (Gatan Inc., Pleasanton, CA) applied in the HRTEM, which is

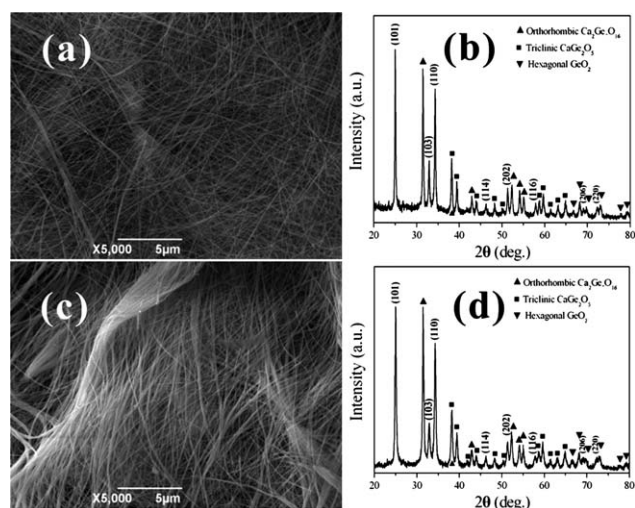


Fig. 3 (a) SEM image of the calcium germanate nanowires obtained from 180 °C for 24 h using the raw materials, with a mole ratio of Ca : Ge = 2 : 7. (b) The corresponding XRD pattern of (a). (c) SEM image of the calcium germanate nanowires obtained from 180 °C for 24 h using raw materials with a mole ratio of Ca : Ge = 1 : 2. (d) The corresponding XRD pattern of (c).

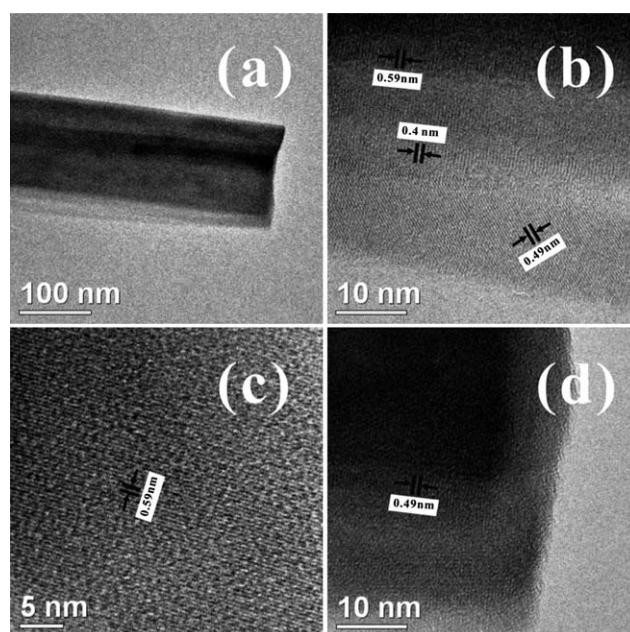


Fig. 5 (a) TEM image of single calcium germanate nanowire. (b) HRTEM image at the edge of the calcium germanate nanowire. (c) HRTEM image in the inner part of the calcium germanate nanowire. (d) HRTEM image at the tip of the calcium germanate nanowire.

the same as the interplanar spacing for the {002} plane of orthorhombic Ca_2GeO_4 , the {111} plane of orthorhombic $\text{Ca}_2\text{Ge}_7\text{O}_{16}$ and the {011} plane of triclinic CaGe_2O_5 , respectively. The interplanar spacing of the crystals at the inner part and tip of the calcium germanate nanowire is about 0.59 nm (Fig. 5c) and 0.49 nm (Fig. 5d), which correspond to the {002} plane of orthorhombic Ca_2GeO_4 and {011} plane of triclinic CaGe_2O_5 , respectively. The results show that all three phases are present in a single calcium germanate nanowire with the phase distribution of orthorhombic Ca_2GeO_4 , orthorhombic $\text{Ca}_2\text{Ge}_7\text{O}_{16}$ and triclinic CaGe_2O_5 structures from the inner part to edge of the calcium germanate nanowires.

The FTIR spectrum at 450–4000 cm^{-1} for the calcium germanate nanowires synthesized under the hydrothermal conditions of 180 °C for 24 h is shown in Fig. 6. This clearly shows a broad absorption at 2800–3800 cm^{-1} , with the absorption peak at 3457.74 cm^{-1} corresponding to the characteristic stretching vibration of hydroxylate (–OH). Peaks localized at 1614.13 cm^{-1} , 1436.71 cm^{-1} and 1027.87 cm^{-1} , respectively, are assigned to asymmetrical and symmetrical stretching vibrations of carboxylate ($\text{O}-\text{C}=\text{O}$), originating from the CH_3COO^- residue in the product. The intensity of the absorption peaks at 715–861 cm^{-1} is associated with the vibration mode B_{2u} and A_g , fundamental to Ge–O bonding.²⁴ The strong absorption peak at 746.32 cm^{-1} is attributed to Ge–O bonding of the calcium germanate nanowires. It is well known that the hexagonal GeO_2 exhibits a typical absorption peak within the wavenumber region from 587 to 516 cm^{-1} and 880.21 cm^{-1} .^{25–28} The peaks at 869.74 cm^{-1} and 576.61 cm^{-1} are considered to be contributed to from the O–Ge–O deformed vibrations with fourfold coordinated germanium of the residue GeO_2 in the calcium germanate nanowires.

The dependence of different growth conditions, such as hydrothermal temperature, reaction time, compactness, Ca source materials and surfactants, on the morphologies and sizes of the calcium germanate nanowires have been analyzed in detail so as to discuss the possible formation process of the calcium germanate nanowires. Fig. 7 shows the time dependence on the formation of the calcium germanate nanowires under different

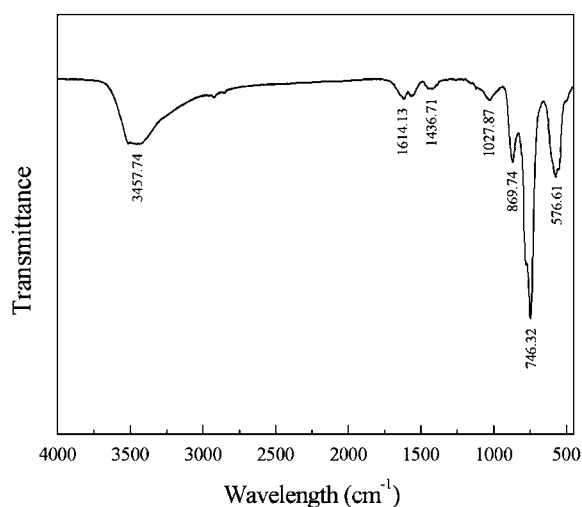


Fig. 6 FTIR spectra of the calcium germanate nanowires synthesized from the hydrothermal conditions of 180 °C for 24 h.

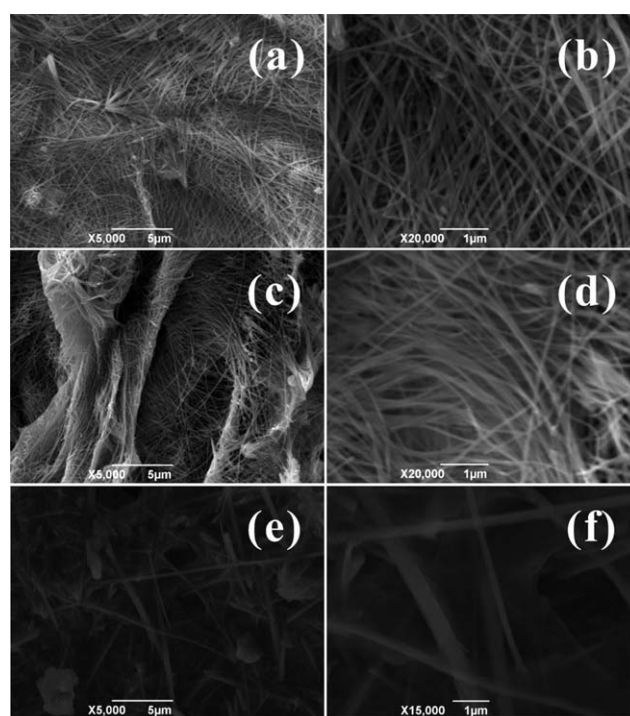


Fig. 7 Time dependence on the formation of the calcium germanate nanowires synthesized at 180 °C for different times. (a) and (b) 12 h, (c) and (d) 6 h, (e) and (f) 0.5 h.

hydrothermal conditions. Calcium germanate nanowires with similar morphology and size can still be obtained when the reaction time decreases to 12 h, 6 h and 0.5 h at 180 °C, respectively. However, the length of the nanowires decreases obviously with the growth time decreasing to 0.5 h and some of the starting materials remain in the products. The time dependence results show that the growth time promotes the growth of the calcium germanate nanowires. Fig. 8 shows the XRD patterns of the calcium germanate nanowires synthesized from 180 °C for 0.5 h, 6 h and 12 h. At the different growth periods of

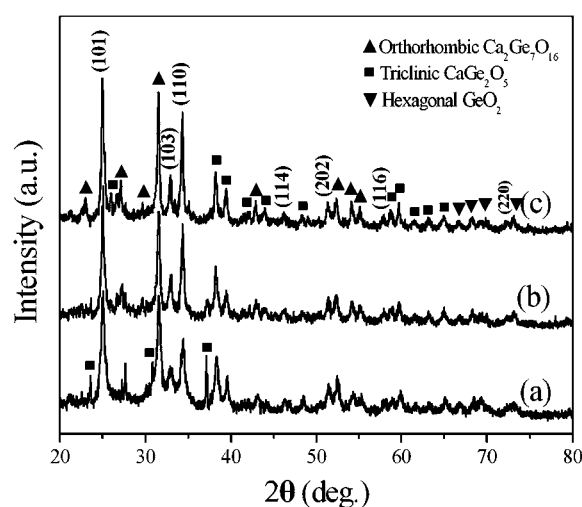


Fig. 8 XRD patterns of the calcium germanate nanowires synthesized at 180 °C for different times. (a) 0.5 h, (b) 6 h, (c) 12 h.

the calcium germanate nanowires, the XRD patterns of the products are similar. However, the intensity of the diffraction peaks of orthorhombic Ca_2GeO_4 and orthorhombic $\text{Ca}_2\text{Ge}_7\text{O}_{16}$ phases increases obviously with an increase in reaction time. The intensity of some diffraction peaks of the triclinic CaGe_2O_5 phase decreases, some diffraction peaks even disappear, such as $2\theta = 24.3^\circ$, 32° and 37.7° . These results demonstrate that a longer reaction time improves the crystalline degree of the nanowires and decreases the content of the triclinic CaGe_2O_5 phase during the growth process of the calcium germanate nanowires.

Fig. 9 displays the effect of the temperature on the formation and growth of calcium germanate nanowires. Obviously, the clustered-shaped calcium germanate nanowires with similar morphology and size (Fig. 9a and b) have been obtained under the hydrothermal conditions of 120°C for 24 h. However, with the temperature further decreasing to 80°C , only microscale cluster-shaped structures composed of short nanorods (Fig. 9c and d) are observed in the product. The diameter and length of this kind of short nanorods are less than 100 nm and about 1 micrometre, respectively. These kind of nanorods are considered to be the precursor of the calcium germanate nanowires. Fig. 10 shows the XRD patterns of the calcium germanate nanowires synthesized from 80°C and 120°C , respectively, for 24 h. Obviously, the intensity of the diffraction peaks increases sharply with an increase in reaction temperature. However, the XRD patterns of the products remain similar. The results demonstrate that the three phases with orthorhombic Ca_2GeO_4 , orthorhombic $\text{Ca}_2\text{Ge}_7\text{O}_{16}$ and triclinic CaGe_2O_5 structures form at the initial formation stage of the calcium germanate nanowires and temperature plays an essential role in the formation of highly crystalline calcium germanate nanowires.

With the increase of the hydrothermal temperature and growth time, the nanorods grow continuously, forming the calcium germanate nanowires. Therefore, the calcium germanate nanowires are believed to originate from the nanorods. It is considered that the nucleation and initial growth process play important roles at the initial reaction stage of GeO_2 and $\text{Ca}(\text{CH}_3\text{COO})_2$. In addition, the growth mechanism of the calcium

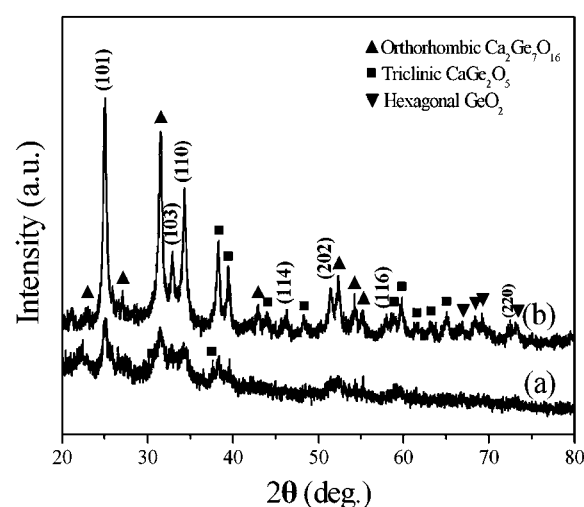


Fig. 10 XRD patterns of the calcium germanate nanowires synthesized at different temperature for 24 h. (a) 120°C , (b) 80°C .

germanate nanowires is also considered to be dominated by a diffusion controlled process, since hydrothermal temperature and growth time play an important role in the formation and growth of the calcium germanate nanowires with the mixed germanate phases. Therefore, the formation of the calcium germanate nanowires is believed to be a combination process of the nucleation and diffusion controlled process.^{29,30}

The pressure originated from the vaporization of water in the autoclave may influence the formation of the calcium germanate nanowires. The pressure is determined by the volume ratio of water in the autoclave which is called compactness. Therefore, the influence of the compactness on the formation of the calcium germanate nanowires are analyzed. The corresponding SEM observation results are shown in Fig. 11. Calcium germanate nanowires with similar morphology and size have also been synthesized from the hydrothermal conditions of 180°C for 24 h when the compactness of autoclave is 80 vol.% (Fig. 11a and b) and 20 vol.% (Fig. 11c and d), respectively. The results show that

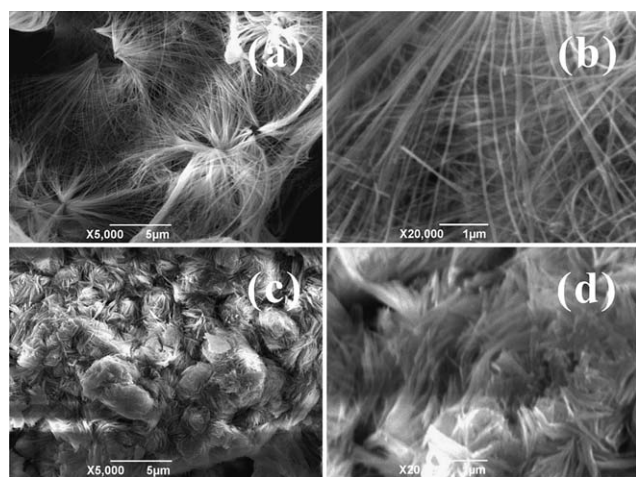


Fig. 9 Temperature dependence on the formation of the calcium germanate nanowires synthesized at different temperatures for 24 h. (a) and (b) 120°C , (c) and (d) 80°C .

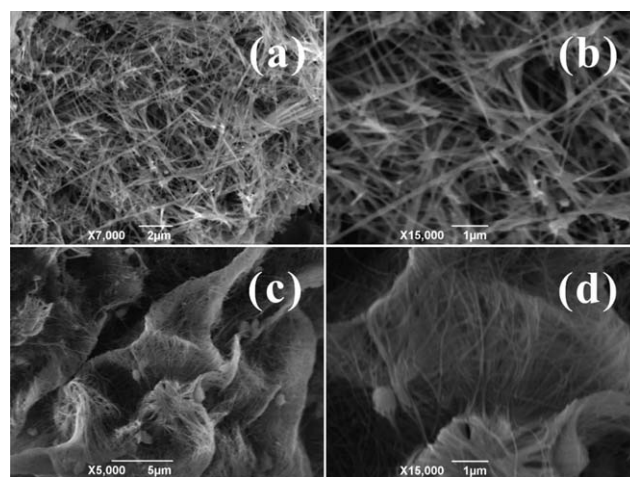


Fig. 11 Compactness dependence on the formation of the calcium germanate nanowires under the hydrothermal conditions of 180°C for 24 h. (a) and (b) 80 vol.% compactness, (c) and (d) 20 vol.% compactness.

the compactness has almost no role on the formation of the calcium germanate nanowires. The calcium germanate nanowires may be obtained easily.

The synthetic process of the calcium germanate nanowires is free of any surfactants. Based on the above discussion, the nucleation, diffusion controlled process and initial growth process exists at the initial reaction stage of GeO_2 and $\text{Ca}(\text{CH}_3\text{COO})_2$. The nanowires grow continuously with the increase in hydrothermal temperature and reaction time. The basic reaction and formation process for the calcium germanate nanowires are proposed to be expressed as follows, according to the nucleation, diffusion controlled process and crystalline growth mechanism. Before hydrothermal treatment, GeO_2 dissolves in water to form H_2GeO_3 solution. At the early stage of the hydrothermal reaction (0.5 h), the reaction between Ca^{2+} and H_2GeO_3 yield calcium germanate cores which are metastable in the reaction system, possibly due to their low crystallinity. Therefore, the calcium germanate crystals with different phases precipitate from the calcium germanate cores, forming short nanorods. With the reaction proceeding (0.5–24 h), the calcium germanate cores are consumed completely and Ca^{2+} and GeO_3^{2-} diffuse into calcium germanate nanowires. Finally, only calcium germanate nanowires exist in the resulting products.

The formation and size of the calcium germanate nanowires can also be controlled by the Ca source materials and surfactants. Fig. 12 shows SEM images of the products obtained from the different Ca source material and surfactants under the hydrothermal conditions of 180 °C for 24 h. Obviously, calcium germanate nanowires have been formed using CaO as the Ca

source material (Fig. 12a). However, almost no nanowires are observed from the product synthesized using CaF_2 as the Ca source material (Fig. 12b). $\text{Ca}(\text{CH}_3\text{COO})_2$ and CaO are easy to dissolved in the water, but CaF_2 is difficult to dissolved in water. Therefore, it is difficult to react CaF_2 with H_2GeO_3 , originating from the GeO_2 and water, to form calcium germanate crystals. The results show that the solvable Ca source material has an important role in the formation of the calcium germanate nanowires. The size of the calcium germanate nanowires can be controlled by adjusting the species of the surfactants. Usually, surfactants are favourable for the formation of one-dimensional nanostructures and tune the size of the one-dimensional nanostructures.^{16,31} It is found that calcium germanate nanowires can also be synthesized easily using 5 wt.% sodium dodecyl sulfate (SDS) (Fig. 12c and d) and ethylenediamine (Fig. 12e and f) as the surfactant at 180 °C for 24 h. However, the diameter of the nanowires synthesized using SDS as the surfactant increases obviously compared with that of the nanowires synthesized without adding any surfactant. The diameter is about 200–400 nm. But the size of the nanowires synthesized using ethylenediamine as the surfactant is similar to those of the nanowires synthesized without adding any surfactant. Therefore, the formation and size of the calcium germanate nanowires may be tuned by adjusting the species of the Ca source materials and surfactants.

The reason that the SDS results in large nanowire diameter and ethylenediamine gives a similar size to those without surfactant is analyzed. Fig. 13 shows the XRD patterns of the calcium germanate nanowires synthesized at 180 °C for 24 h using different surfactants. Obviously, the XRD pattern of the calcium germanate nanowires obtained using ethylenediamine as the surfactant is almost the same as that of the germanate nanowires obtained without surfactants. However, the main phase of the products obtained using SDS as the surfactant is a monoclinic $\text{Na}_2\text{Ge}_2\text{O}_5$ structure (JCPDS card No. 34-1290) besides orthorhombic Ca_2GeO_4 , orthorhombic $\text{Ca}_2\text{Ge}_2\text{O}_{16}$ and triclinic CaGe_2O_5 structures. The $\text{Na}_2\text{Ge}_2\text{O}_5$ phase originates

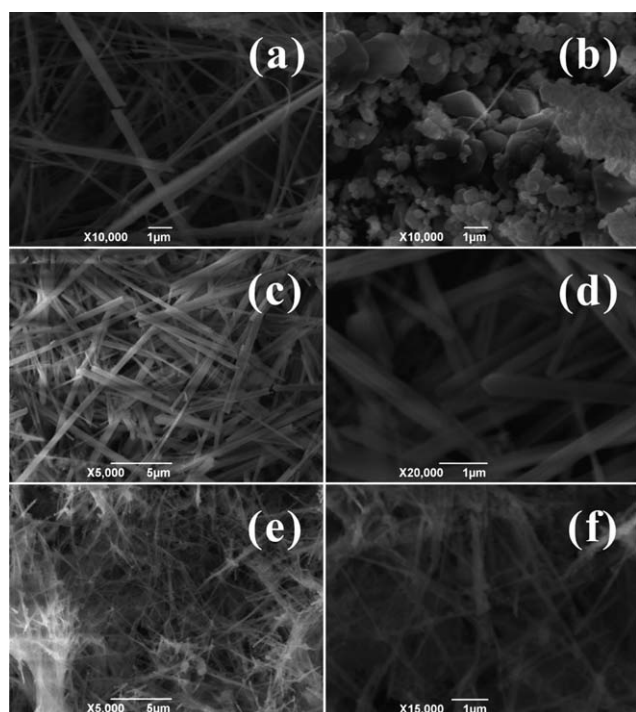


Fig. 12 Ca source material and surfactant dependencies on the formation of the calcium germanate nanowires under the hydrothermal conditions of 180 °C for 24 h. (a) CaO as the Ca source material, (b) CaF_2 as the Ca source material, (c) and (d) SDS as the surfactant, (e) and (f) ethylenediamine as the surfactant.

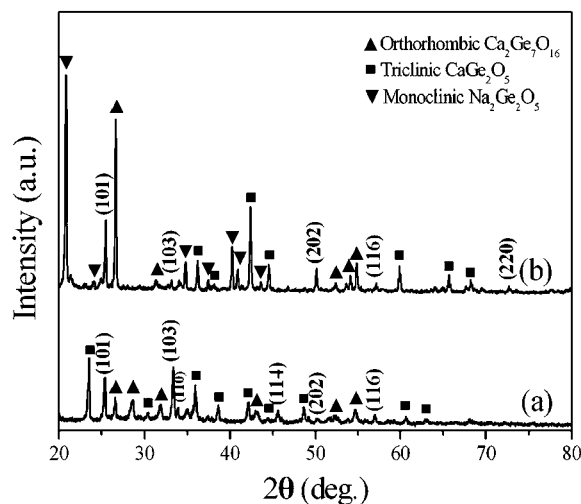


Fig. 13 XRD patterns of the calcium germanate nanowires synthesized at 180 °C for 24 h using different surfactants: (a) ethylenediamine; (b) SDS.

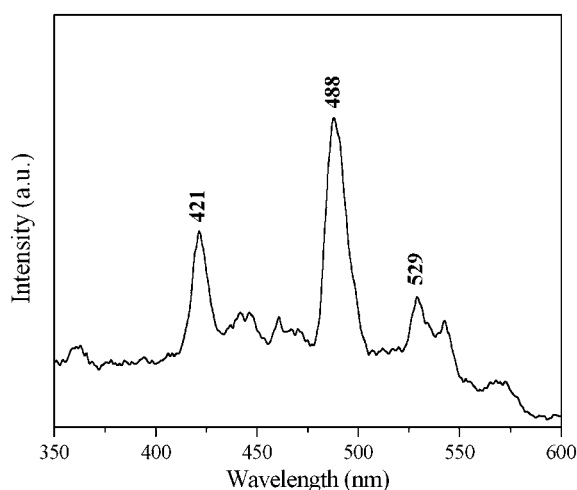


Fig. 14 PL spectrum of the calcium germanate nanowires.

from the reaction of H_2GeO_3 and Na^+ in SDS resulting the increase of the diameter of the nanowires.

The optical properties of the calcium germanate nanowires have been analyzed by PL to further assess their quality. Fig. 14 is the room temperature PL spectrum of the calcium germanate nanowires synthesized at 180°C for 24 h, exhibiting strong blue light emission centered at 421 nm and 488 nm, and a poor green light emission centered at 529 nm. The blue light PL emission peak at 420 nm have been observed in α -quartz after Ge^+ implantation at elevated temperature³² and amorphous $\text{Ca}_5\text{Ge}_2\text{O}_9$ nanowires,²¹ respectively, which is considered to be caused by the Ge-related defect center. The PL emission peak at 421 nm in Fig. 14 is very close to the above literature showing the same PL emission origin. Blue light emission has been reported from one-dimensional GeO_2 nanostructures.^{33–36} The intensive PL peak at 488.5 nm and 476 nm for the GeO_2 nanowires and chain-like structures were observed, respectively.^{28,35} The blue luminescence is believed to originate from the radiative recombination between an electron on oxygen vacancies (V_{O}^\bullet) and a hole on oxygen–germanium vacancies centers ($(V_{\text{O}}^\bullet, V_{\text{Ge}}^\bullet)$). Moreover, the similar blue light PL emission peak at about 488 nm have been observed in other one-dimensional germanate nanomaterials, such as strontium germanate nanowires,¹⁸ amorphous $\text{Ca}_5\text{Ge}_2\text{O}_9$ ²² and chain-like $\text{In}_2\text{Ge}_2\text{O}_7$ /amorphous GeO_2 core/shell nanocables.³⁷ The results show that the blue light PL emission spectrum from the calcium germanate nanowires is relative to Ge rather than to Ca. Therefore, Ca in the calcium germanate nanowires does not have an effect on the PL emission ability. The green emission bands at 530 nm and 532 nm for zinc germanate nanostructures³⁸ and CuGeO_3 nanowires²³ were reported, which is attributed to Ge-associated luminescence centers. Based on the above analysis, the luminescence of the calcium germanate nanowires is believed to be originated from the Ge-associated luminescence centers.

Conclusions

In summary, crystalline calcium germanate nanowires have been synthesized via a simple and facile hydrothermal route using GeO_2 and $\text{Ca}(\text{CH}_3\text{COO})_2 \cdot \text{H}_2\text{O}$ as the starting materials in the

absence of any surfactant. The calcium germanate nanowires with flat tips and smooth surface have a diameter of 50–200 nm and length of several dozens of micrometres, even longer than 100 μm . The growth conditions, such as reaction temperature, reaction time, compactness, Ca source materials and surfactants, have important effects on the formation and size of the calcium germanate nanowires. The fluorescence emission peaks centered at 421 nm, 488 nm and 529 nm are observed in the room temperature photoluminescence measurements. It is believed that the synthesis route might provide a new possibility for synthesizing other species of nanowires.

Acknowledgements

This work was supported by the Natural Science Foundation of the Education Bureau of Anhui Province of China (KJ2011A042), Innovative Research Foundation of Postgraduate of Anhui University of Technology (2010008) and the Program for New Century Excellent Talents in University of China (NCET-08-0618).

References

- 1 C. Y. Yan, P. S. Lee, *Nanoelectronics Conference (INEC)*, 2010 3rd International, Hong Kong, P.R. China, 2010, 3–8, 48–49.
- 2 Y. B. Mao, T. J. Park and S. S. Wong, *Chem. Commun.*, 2005, **14**, 5721–5735.
- 3 G. Z. Shen, P. C. Chen, K. Ryu and C. W. Zhou, *J. Mater. Chem.*, 2009, **19**, 828–839.
- 4 C. L. Jiang, K. Kiyofumi, Y. F. Wang and K. Koumoto, *Cryst. Growth Des.*, 2007, **7**, 2713–2715.
- 5 Z. S. Hong, M. D. Wei, Q. X. Deng, X. K. Ding, L. L. Liang and K. M. Wei, *Chem. Commun.*, 2010, **46**, 740–742.
- 6 C. Pang, B. Yan, L. Liao, B. Liu, Z. Zheng, T. Wu, H. D. Sun and T. Yu, *Nanotechnology*, 2010, **21**, 465706.
- 7 Y. Su, L. Zhu, L. Xu, Y. Q. Chen, H. H. Xiao, Q. T. Zhou and Y. Feng, *Mater. Lett.*, 2007, **61**, 351–354.
- 8 D. L. Young, D. L. Williamson and T. J. Coutts, *J. Appl. Phys.*, 2002, **91**, 1464–1471.
- 9 A. Wang, J. Dai, J. Cheng, M. P. Chudzik, T. J. Marks, R. P. H. Chang and C. R. Kannewurf, *Appl. Phys. Lett.*, 1998, **73**, 327–330.
- 10 J. S. Jie, G. Z. Wang, X. H. Han, J. P. Fang, Q. X. Yu, Y. Liao, B. Xu, Q. T. Wang and J. G. Hou, *J. Phys. Chem. B*, 2004, **108**, 8249–8253.
- 11 J. H. Huang, X. C. Wang, Y. D. Hou, X. F. Chen, L. Wu and X. Z. Fu, *Environ. Sci. Technol.*, 2008, **42**, 7387–7391.
- 12 G. Z. Liu, S. T. Zheng and G. Y. Yang, *Angew. Chem., Int. Ed.*, 2007, **46**, 2827–2830.
- 13 S. S. Bayya, G. D. Chin, J. S. Sanghera and I. D. Aggarwal, *Opt. Express*, 2006, **14**, 11687–11693.
- 14 Y. P. Dong, L. Z. Pei, X. F. Chu, W. B. Zhang and Q. F. Zhang, *Electrochim. Acta*, 2010, **55**, 5135–5141.
- 15 C. Y. Yan and P. S. Lee, *J. Phys. Chem. C*, 2009, **113**, 14135–14139.
- 16 C. Y. Yan, N. D. Singh and P. S. Lee, *Appl. Phys. Lett.*, 2010, **96**, 053108.
- 17 N. Wang, J. Ding, G. C. Li and H. R. Peng, *Cryst. Res. Technol.*, 2010, **45**, 316–320.
- 18 M. Y. Tsai, T. P. Perng, *The 214th Electrochemical Society Meeting*, Honolulu, HI, USA 2008, 12–17.
- 19 L. Z. Pei, H. S. Zhao, W. Tan, H. Y. Yu, Y. W. Chen and Q. F. Zhang, *CrystEngComm*, 2009, **11**, 1696–1701.
- 20 L. Z. Pei, J. F. Wang, W. Tan, H. Y. Yu, C. G. Fan, J. Chen and Q. F. Zhang, *Curr. Nanosci.*, 2009, **5**, 470–473.
- 21 M. Y. Sharonov, A. B. Bykov, T. Myint, V. Petricevic and R. R. Alfano, *Opt. Commun.*, 2007, **275**, 123–128.
- 22 M. Y. Tsai, C. Y. Yu and T. P. Perng, *J. Nanosci. Nanotechnol.*, 2008, **8**, 6376–6380.

- 23 L. Z. Pei, J. F. Wang, L. J. Yang, Y. P. Dong, S. B. Wang, C. G. Fan, J. L. Hu and Q. F. Zhang, *Crystal Research and Technology*, 2011, **46**, 103–112.
- 24 S. D. Devic, M. J. Konstantinovic, Z. V. Popovic, G. Dhalenne and A. Revcolevschi, *J. Phys.: Condens. Matter*, 1994, **6**, L745–L753.
- 25 C. B. Jing, J. X. Hou and X. G. Xu, *Opt. Mater.*, 2008, **30**, 857–859.
- 26 Y. Kanno and J. Nishino, *J. Mater. Sci. Lett.*, 1993, **12**, 110–115.
- 27 K. Blaszcak, W. Jelonek and A. Adamczyk, *J. Mol. Struct.*, 1999, **511–512**, 163–166.
- 28 L. Z. Pei, H. S. Zhao, W. Tan and Q. F. Zhang, *J. Appl. Phys.*, 2009, **105**, 054313.
- 29 A. Katsman, Y. Yaish, E. Rabkin and M. Beregovsky, *J. Electron. Mater.*, 2010, **29**, 365–370.
- 30 V. G. Dubrovskii, N. V. Sibirev, R. A. Suris, G. E. Cirlin, J. C. Harmand and V. M. Ustinov, *Surf. Sci.*, 2007, **601**, 4395–4401.
- 31 M. H. Cao, Y. H. Wang, Y. J. Qi, C. X. Guo and C. W. Hu, *J. Solid State Chem.*, 2004, **177**, 2205–2209.
- 32 P. K. Sahoo, S. Dhar, S. Gasiorek and K. P. Lieb, *J. Appl. Phys.*, 2004, **96**, 1392–1397.
- 33 Y. H. Tang, Y. F. Zhang, N. Wang, I. Bello, C. S. Lee and S. T. Lee, *Appl. Phys. Lett.*, 1999, **74**, 3824–3826.
- 34 K. P. Kalyanikutty, G. Gundiah, A. Govindaraj and C. N. Rao, *J. Nanosci. Nanotechnol.*, 2005, **5**, 421–424.
- 35 Y. Su, Z. Y. He, Y. Q. Chen, J. Jiang, D. Cai and L. Chen, *Mater. Lett.*, 2005, **59**, 2990–2993.
- 36 Y. Su, X. M. Liang, S. Li, Y. Q. Chen, Q. T. Zhou, S. Yin, X. Meng and M. G. Kong, *Mater. Lett.*, 2008, **62**, 1010–1013.
- 37 Y. Su, X. Meng, S. Li, Y. Q. Chen, L. Xu, Q. T. Zhou, S. Yin, B. Peng, X. M. Liang and Y. Feng, *J. Nanosci. Nanotechnol.*, 2007, **7**, 4365–4368.
- 38 L. Li, Y. Su, Y. Q. Chen, M. Gao, Q. Chen and Y. Feng, *Adv. Sci. Lett.*, 2010, **3**, 1–5.